

## **Carbon Nanofibers with Inter-bonded Fibrous Structure for Supercapacitor Application**

Haitao Niu, Xungai Wang, Tong Lin\*

*Institute for Frontier Materials Deakin University, Geelong, VIC 3217, Australia*  
Email: [tong.lin@deakin.edu.au](mailto:tong.lin@deakin.edu.au)

### **Abstract**

In this study, we have improved carbon nanofiber interconnection by using two electrospinning methods: conventional electrospinning and side-by-side bicomponent electrospinning to produce polyvinylpyrrolidone (PVP)/polyacrylonitrile (PAN) blend nanofibers and PVP/PAN side-by-side bicomponent nanofibers respectively. Upon carbonization, the nanofibers showed inter-bonded morphologies. PVP here functioned to bind nanofibers during carbonization. The inter-bonded fibrous morphology was highly affected by the PVP/PAN ratio and the electrospinning method. Carbon nanofibers prepared by the bicomponent electrospinning were found to have larger capacitances compared to those prepared by the conventional electrospinning. The influence of electrospinning method, PAN/PVP ratio on the crystallinity of carbon nanofibers, their surface morphology and capacitor performance were examined. The influence mechanism was elucidated as well.

### **1. INTRODUCTION**

Supercapacitors are important electrochemical energy storage devices having wide applications in areas such as consumer electronics, memory back-up systems, industrial power and energy management (Zhang 2009). They have extremely high power density and can be charged and discharged quickly and repeatedly for a long time without degradation. Supercapacitors often serve to fill the gap between batteries and conventional capacitors (Simon 2008). To achieve high capacitance values, carbon supercapacitor electrode materials are usually featured with large surface areas (Shi 1996, Kim 2003, Ania 2007, Chmiola 2010, Jurewicz 2006, Chen 2010, Stoller 2008, Wang 2009, Kim 2003, Kim 2004, Kim 2005). Among all the porous carbon electrodes, carbon nanofibers prepared from electrospun polymer precursor nanofibers are relatively new and have not been well explored.

Electrospinning is an effective technique to produce polymeric nanofibers. It is well-known for its easy operation, universality in processing different polymers, ability to control fiber diameter and morphology, and versatility in producing functional nanofibers. The very large surface-to-weight (or volume) ratio and high porosity make carbon nanofibers excellent candidates for electrode materials. Electrospun carbon nanofibers typically have a nonwoven-like fibrous structure (Kim 2003, Kim 2004). For electrochemistry-associated processes, nonwoven structures may have low charge-transfer efficiency because of the insufficient fiber-fiber contact leading to large contact-resistance and prolonged charge-transfer through the electrode

(Pandolfo 2006). The lack of inter-fiber connection may also reduce the pore stability. How to build effective inter-fiber connections among electrospun carbon nanofibers has not been reported in research literatures.

In this study, we demonstrate the production of inter-bonded carbon nanofiber membranes simply by pyrolysis of nanofibers containing PAN, and a thermoplastic polymer polyvinylpyrrolidone (PVP) serving as a binding agent. Two electrospinning techniques: conventional electrospinning and bicomponent electrospinning were used to produce PVP/PAN blend nanofibers and side-by-side bicomponent nanofibers, respectively. The effects of weight ratio of PVP/PAN on the morphologies of the as-spun nanofibers and the resultant carbon fibers, their crystallinity and the capacitances were examined.

## 2. EXPERIMENTAL DETAILS

### 2.1 Materials

Polyvinylpyrrolidone (PVP, Sigma-Aldrich,  $M_w \sim 1,300,000$ ), polyacrylonitrile (PAN, Sigma-Aldrich,  $M_w \sim 86,200$ ), N, N'-dimethylformide (DMF, Sigma-Aldrich), high purity nitrogen (4.0, Migomag) and carbon dioxide (Foodgrade, Migomag) were used as received.

### 2.2 Electrospinning

Side-by-side bicomponent nanofibers were prepared using a purpose-made micro-fluidic electrospinning spinneret developed in our lab. PVP (22 wt%) and PAN (10 wt%) solutions were fed separately into the inlet channels of the spinneret which combined into an outlet channel to form a laminar flow. The weight ratio of PVP/PAN was controlled by their flow rates. PVP/PAN blend nanofibers were prepared by a conventional electrospinning setup using PVP/PAN solution mixture (with the same flow rate to that in side-by-side electrospinning). Five different weight ratios (33/67, 43/57, 68/32, 87/13 and 92/8) of PVP/PAN solutions were investigated in side-by-side and blend electrospinning, respectively. The applied voltage and the electrospinning distance were controlled at 20 kV and 15 cm, respectively.

### 2.3 Pyrolysis of nanofibers

The pyrolysis of nanofibers was performed in a tubular furnace (TF55035C-1, Lindberg/Blue M) under the following condition: room temperature to 300 °C (2 hrs /air), 300 °C to 500 °C (2 hrs/ $N_2$ ), 500 to 970 °C (1 hr/ $N_2$ ). The carbonized nanofibers were activated by  $CO_2$  at 850 °C for 1.5 hrs directly after carbonization.

### 2.4 Characterizations

The fiber morphologies were observed on a scanning electron microscope (SEM Supra 55VP) and a transmission electron microscope (JEM-2100). Raman spectra were measured on a 633 Argon ion laser/Renishaw Invia spectrograph. Wide angle X-ray diffraction (WXR) measurements were performed on a powder diffractometer (Philips 1140/90) using Cu K $\alpha$  radiation of wavelength 1.54 Å. The surface area of carbon nanofiber membranes were measured using the B.E.T. nitrogen adsorption method in Quantachrome Autosorb-1 instrument.

Electrochemical capacitance of carbon nanofiber membranes were measured using a cyclic voltammetry method on an electrochemistry workstation (EChem V2.0.7). A typical three-electrode cell was employed with the carbon nanofiber

membrane ( $300 \pm 20 \mu\text{m}$  in thickness) as working electrode, a platinum foil as the counter electrode and Ag/AgCl as the reference electrode. 1.0 M  $\text{H}_2\text{SO}_4$  aqueous solution was used as the electrolyte solution. The measurement was performed at room temperature, with the scan range of  $-0.1 \sim 0.9 \text{ V}$  and scan rate of  $5 \text{ mV/s}$ .

### 3. RESULTS AND DISCUSSIONS

Side-by-side bicomponent nanofibers were prepared using a purpose-made micro-fluidic electrospinning spinneret shown in **Fig. 1a** (Lin 2005). PVP (22 wt%) and PAN (10 wt%) solutions were fed separately into the inlet channels of the spinneret which converged into the outlet channel. Electrospinning of the fluid at the outlet channel end resulted in side-by-side bicomponent nanofibers. The morphology of the PVP/PAN side-by-side nanofibers is shown in **Fig. 1b**, the nanofibers have a straight fibrous structure. To verify the side-by-side bicomponent configuration, the PVP component was removed by ethanol extraction, the remaining PAN showed a “C” shaped cross-section (**Fig. 1c**). The inset TEM image in **Fig. 1c** also proves this morphology. For comparison, PVP/PAN blend nanofibers, electrospun using a conventional needle electrospinning setup (Lin 2004), have a uniform fibrous structure with a circular cross-section (**Fig. 1d**). Dissolving the PVP composition from the blend nanofibers resulted in a porous fiber structure (**Fig. 1e**). The electrospinning modes and polymer composition had little influence on the average fiber diameter. When the PVP/PAN ratios were 43/57 and 68/32 (wt/wt), both the side-by-side and the blend nanofibers had the same average diameters. Slightly coarser bicomponent nanofibers were obtained when the PVP/PAN ratios were 33/67, 87/13, and 92/8

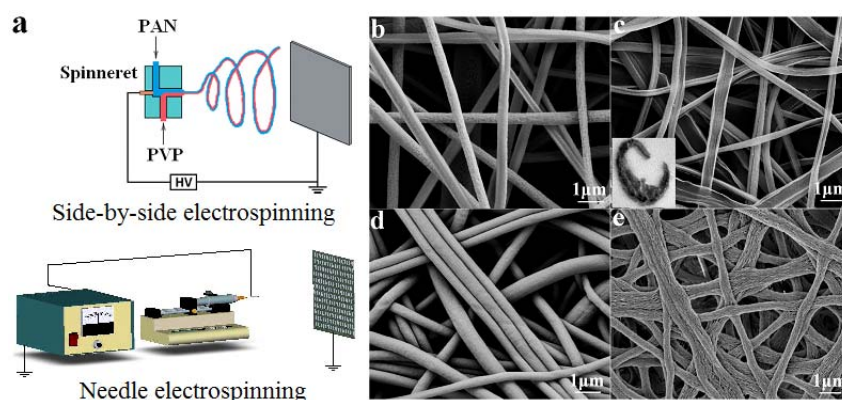


**Fig. 1** a) Apparatus for side-by-side electrospinning (top) and needle electrospinning (bottom), b~e) SEM images of electrospun PVP/PAN nanofibers (PVP/PAN ratio = 68/32 wt/wt). b) Side-by-side PVP/PAN nanofibers, c) Side-by-side PVP/PAN nanofibers with the PVP component removed (inset TEM image of the cross-sectional view), d) Blend PVP/PAN nanofibers, e) Blend PVP/PAN nanofibers with the PVP component removed.

The carbonized PVP/PAN nanofibers varied considerably in the fiber morphology depending on the electrospinning mode and PVP/PAN ratio (**Fig. 2**). In this work, the carbon nanofibers prepared from side-by-side nanofibers with the PVP/PAN weight ratios of 33/67, 43/57, 68/32, 87/13, and 92/8 for electrospinning are named as

samples S-CNF01, S-CNF02, S-CNF03, S-CNF04 and S-CNF05, respectively. It is interesting to note that the resulting carbon fibers maintained their original fibrous structure in most parts when the PVP content in the precursor was low, except that some fiber-fiber interconnections (circled areas) occurred at the intersection areas (S-CNF01 and S-CNF02). With the increased PVP content, the fiber-fiber interconnections became apparent (S-CNF03). When the PVP content was further increased, fibers started to merge around the fiber-fiber intersection areas (S-CNF04) and the fiber uniformity became worse. Higher PVP content in the precursor fibers led to a highly inter-bonded fibrous structure (S-CNF05). The carbon nanofibers produced from PVP/PAN blend nanofibers, which are named as B-CNFs, were more uniform, but less interconnected (**Fig. 2**). At a low PVP content (e.g. samples B-CNF01 and B-CNF02), there were almost no fiber-fiber interconnections in the samples. Interconnections became obvious when the precursor contained higher PVP contents (e.g. samples B-CNF03~05).

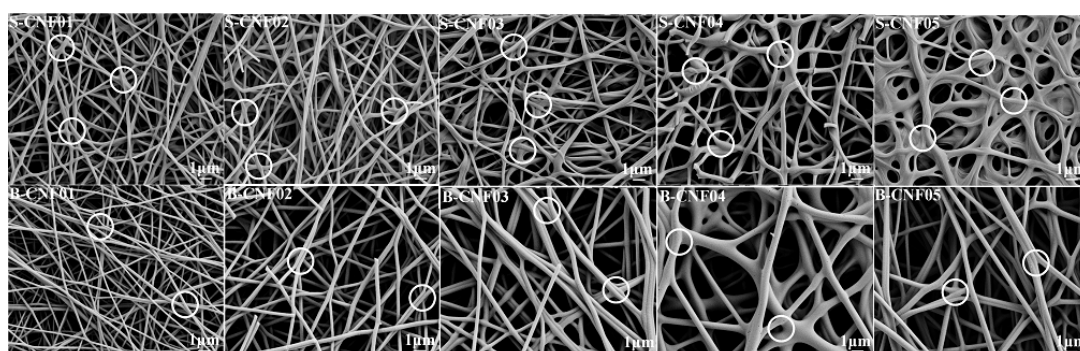


**Fig. 2** SEM images of carbon nanofibers.

The structures of these carbon nanofibers were investigated by Raman and XRD. In the Raman spectra (**Fig. 3a**), all the carbon nanofibers exhibited two characteristic peaks at about  $1580\text{ cm}^{-1}$  and  $1350\text{ cm}^{-1}$ , which were respectively assigned to G and D bands. The G band is associated with  $sp^2$  vibrations of perfect graphite crystal, while the D band corresponds to the vibrations at the crystal 'edges'. The intensity ratio of D and G bands,  $R=I_D/I_G$ , was used to characterize the extent of graphitization and the alignment of the graphitic planes within carbon materials (Kim 2004). Curve-fitting results of these spectra indicated that the lower R values for the carbon nanofibers prepared from the side-by-side PVP/PAN nanofibers (S-CNF03) and pure PAN nanofibers (PAN-C) suggested the greater amount of  $sp^2$  (graphite) clusters in the samples. Since Raman can only detect the area with an optical skin depth (ca. 10 nm) (Kim 2006), the result is meaningful only on the carbon nanofiber surface. The crystalline planar size ( $L_a$ ) was calculated from Raman spectra and shown in Table 1 (Jawhari 1995). The carbon nanofibers from the pure PAN and the side-by-side PVP/PAN nanofibers had larger crystalline planar size and smaller inter-layer space compared to those from PVP/PAN blend and pure PVP nanofibers. Since large crystal plane size and small inter-layer space can facilitate the charge transfer (Pimenta 2007, Fanjul 2004), the carbonized side-by-side nanofibers should have better electrical conductivity than those from blend ones.

X-ray diffraction (XRD) reflects the bulk properties of carbon nanofibers. As shown in **Fig. 3b**, the XRD patterns of carbon nanofibers have two main diffraction peaks at,  $2\theta = 24.2^\circ$  and  $44^\circ$ , corresponding to the graphitic crystallite planes (002)

and (101), respectively (Kim 2004). The inter-layer distance ( $d$ ) within graphite and the overall graphite crystalline thickness  $L_c(002)$  were calculated according to Bragg (Bragg 1913) and Scherrer (Wang 2006) equations, respectively. The calculated  $d$  and  $L_c(002)$  values are also listed in **Table 1**. Carbon nanofibers from PAN typically showed a larger crystallite thickness than those from PVP. The sample B-CNF03 had larger  $L_c$  values than S-CNF03, indicating that carbon nanofibers from polymer blend nanofibers had a larger crystallite thickness. These results suggest that the carbon crystalline around the fiber surface is slightly different from the bulk fibers. Combining the result from Raman and XRD, it is reasonable to conclude that the graphite crystalline in the side-by-side PVP/PAN carbonized carbon fibers has larger sheet size but smaller in thickness compared to those prepared from blended fibers.

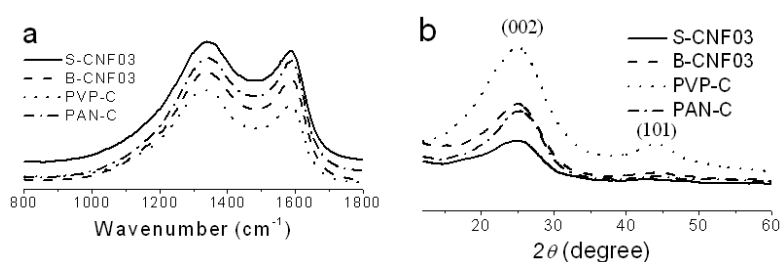


**Fig. 3** a) Raman spectra, and b) XRD patterns of carbon nanofibers.

**Table 1.** Raman and XRD results of carbon nanofibers

Carbon	Raman			XRD		
	Peak (cm <sup>-1</sup> )	Bandwidth (cm <sup>-1</sup> )	ID/IG	La (nm)	d (Å)	Lc (nm)
S-CNF03	D 1335	271	6.88	0.84	3.52	1.11
	G 1594	75				
B-CNF03	D 1337	260	10.11	0.57	3.54	1.18
	G 1597	75				
PVP-C	D 1331	256	10.12	0.57	3.56	0.96
	G 1594	69				
PAN-C	D 1334	259	5.42	1.07	3.52	1.14
	G 1594	71				

**Fig. 4** shows the surface area of carbon nanofiber membranes. The surface area values didn't show monotonic changes with the PVP/PAN ratios and electrospinning methods. The sample S-CNF02 had the largest surface area, which was consistent with the results in the isotherm curves. The surface area values for B-CNF samples were generally smaller than those of the S-CNF counterparts except B-CNF01. The difference between PVP and PAN based carbon nanofibers led to discrepancies in the surface area when the PVP/PAN ratio was changed. The nitrogen absorption/desorption isotherms of carbon nanofibers showed that all carbon nanofibers had microporous and mesoporous characteristics, in spite of the variations in PVP/PAN ratio and electrospinning mode.

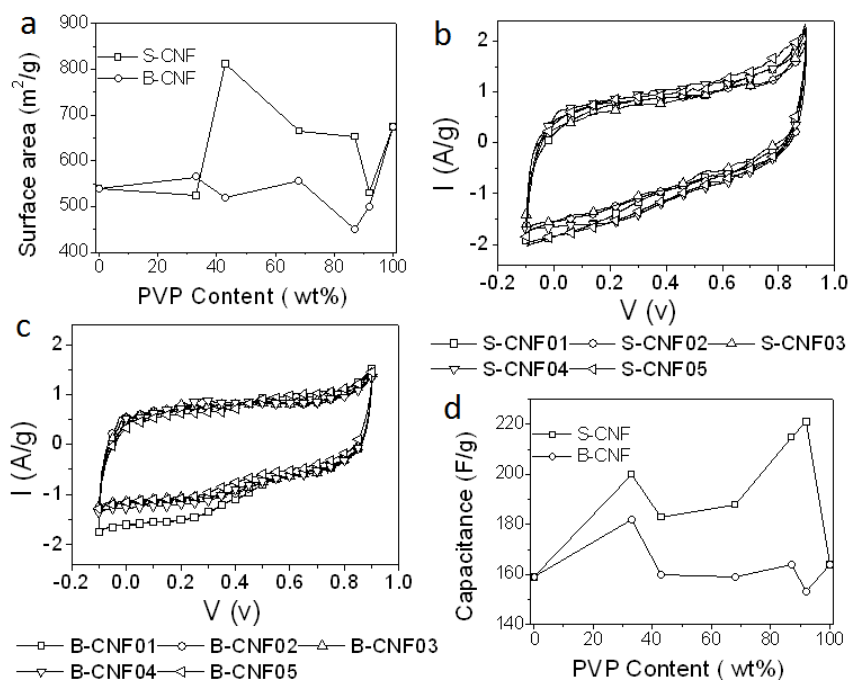


**Fig. 4** a) B.E.T surface area, b) ~ c) CV curves of carbon nanofibers and d) Capacitance values.

The capacitances of carbon nanofiber membranes were measured in a three electrode cell using the electrochemical cyclic voltammetry (CV) method. All carbon fiber membranes had near-rectangular charge/discharge characteristics. The capacitances calculated according to the CV curves are given in **Fig. 4**. B-CNFs generally had smaller capacitance values than S-CNFs. In comparison to those prepared from blending electrospinning and single component electrospinning, the carbon nanofibers prepared from side-by-side PVP/PAN nanofibers showed improved electrochemical capacitances. Depending on the PVP/PAN ratio, the improvement varied from 18 F/g (PVP/PAN = 33/67 wt/wt) to as high as 68 F/g (PVP/PAN = 92/8 wt/wt). Such an improvement indicates the advantage of side-by-side electrospinning. There was, however, no obvious linear relationship between PVP/PAN ratios and capacitive performances. Among all the carbon nanofibers, S-CNF05 has the largest capacitance value (221 F/g), in spite of its relatively smaller surface area (531  $\text{m}^2/\text{g}$ ). It is interesting to note that the capacitance values reported herein are higher than those measured from graphene (135 F/g) (Stoller 2008) and other electrospun carbon nanofibers reported in the literature (e.g. PBI (Kim 2005), polyimide (Kim 2004), PAN (Kim 2003)), which had uniform separated fibrous structures). The inter-bonded carbon fibers prepared from the side-by-side bicomponent fibers have shown several advantages: the pure PAN component maintains the intrinsic fibrous structure after the pyrolysis, whereas the PVP component shrinks to build the fiber interconnections.

## CONCLUSIONS

We have demonstrated that side-by-side nanofibers having PAN on one side and PVP on the other are effective precursors to produce an inter-bonded carbon nanofiber network. The carbon fiber-fiber interconnections have been established

simply by pyrolysis of the precursor fibers which show no inter-fiber connections, and the inter-bonded fiber morphology is determined by the ratio of two polymer components within the fibers. The carbon nanofibers produced from the side-by-side polymer nanofibers show better fiber-interconnections and carbon crystalline structure than those produced from blend nanofibers of the same polymers at the same content. The carbon nanofibers produced from side-by-side polymer nanofibers have larger electrochemical capacitances compared to those prepared from polymer blend ones. Side-by-side nanofibers may serve as an important precursor nanofiber material to produce well inter-bonded carbon nanofibrous network, and these carbon membranes have potential applications not only in supercapacitors but also in Li-ion batteries, fuel cells, splitting of water and many other electrochemical processes.

## REFERENCES

- Ania, C.O., Khomenko, V., Raymundo-Piñero, E., Parra, J.B. and Béguin, F. (2007), "The Large Electrochemical Capacitance of Microporous Doped Carbon Obtained by Using a Zeolite Template." *Advanced Functional Materials*, Vol. **17**, 1828-1836
- Bragg, W.L. (1913), "The Diffraction of Short Electromagnetic Waves by a Crystal." *Proceedings of the Cambridge Philosophical Society*, Vol. **17**, 43-57
- Chen, W., Fan, Z., Gu, L., Bao, X. and Wang, C. (2010), "Enhanced capacitance of manganese oxide via confinement inside carbon nanotubes." *Chemical Communications*, Vol. **46**, 3905-3907
- Chmiola, J., Largeot, C., Taberna, P.-L., Simon, P. and Gogotsi, Y. (2010), "Monolithic Carbide-Derived Carbon Films for Micro-Supercapacitors." *Science*, Vol. **328**, 480-483
- Fanjul, F., Granda, M., Santamaría, R. and Menéndez, R. (2004), "The influence of processing temperature on the structure and properties of mesophase-based polygranular graphites." *Journal of Materials Science*, Vol. **39**, 1213-1220
- Jawhari, T., Roid, A. and Casado, J. (1995), "Raman spectroscopic characterization of some commercially available carbon black materials." *Carbon*, Vol. **33**, 1561-1565
- Jurewicz, K., Babel, K., Pietrzak, R., Delpeux, S. and Wachowska, H. (2006), "Capacitance properties of multi-walled carbon nanotubes modified by activation and ammoxidation." *Carbon*, Vol. **44**, 2368-2375
- Kim, C. and Yang, K.S. (2003), "Electrochemical properties of carbon nanofiber web as an electrode for supercapacitor prepared by electrospinning." *Applied Physics Letters*, Vol. **83**, 1216-1218
- Kim, C. and Yang, K. (2003), "Electrochemical properties of carbon nanofiber web as an electrode for supercapacitor prepared by electrospinning." *Applied Physics Letters*, Vol. **83**, 1216
- Kim, C., Choi, Y.-O., Lee, W.-J. and Yang, K.-S. (2004), "Supercapacitor performances of activated carbon fiber webs prepared by electrospinning of PMDA-ODA poly(amic acid) solutions." *Electrochimica Acta*, Vol. **50**, 883-887
- Kim, C. (2005), "Electrochemical characterization of electrospun activated carbon nanofibres as an electrode in supercapacitors." *Journal of Power Sources*, Vol. **142**, 382-388
- Kim, C., *et al.* (2004), "Raman spectroscopic evaluation of polyacrylonitrile-based carbon nanofibers prepared by electrospinning." *Journal of Raman Spectroscopy*, Vol. **35**, 928-933
- Kim, C., *et al.* (2006), "Fabrication of electrospinning-derived carbon nanofiber webs for the anode material of lithium-ion secondary batteries." *Advanced Functional Materials*, Vol. **16**, 2393-2397

- Lin, T., Wang, H. and Wang, X. (2005), "Self-Crimping Bicomponent Nanofibers Electrospun from Polyacrylonitrile and Elastomeric Polyurethane." *Advanced Materials*, Vol. **17**, 2699-2703
- Lin, T., Wang, H., Wang, H. and Wang, X. (2004), "The charge effect of cationic surfactants on the elimination of fibre beads in the electrospinning of polystyrene." *Nanotechnology*, Vol. **15**, 1375–1381
- Pandolfo, A.G. and Hollenkamp, A.F. (2006), "Carbon properties and their role in supercapacitors." *Journal of Power Sources*, Vol. **157**, 11-27
- Pimenta, M.A., *et al.* (2007), "Studying disorder in graphite-based systems by Raman spectroscopy." *Physical Chemistry Chemical Physics*, Vol. **9**, 1276-1290
- Shi, H. (1996), "Activated carbons and double layer capacitance." *Electrochimica Acta*, Vol. **41**, 1633-1639
- Simon, P. and Gogotsi, Y. (2008), "Materials for electrochemical capacitors." *Nature Materials*, Vol. **7**, 845-854
- Stoller, M.D., Park, S., Zhu, Y., An, J. and Ruoff, R.S. (2008), "Graphene-Based Ultracapacitors." *Nano Letters*, Vol. **8**, 3498-3502
- Wang, S., Chen, Z.H., Ma, W.J. and Ma, Q.S. (2006), "Influence of heat treatment on physical–chemical properties of PAN-based carbon fiber." *Ceramics International*, Vol. **32**, 291-295
- Wang, Y., *et al.* (2009), "Supercapacitor devices based on graphene materials." *Journal of Physical Chemistry C*, Vol. **113**, 13103-13107
- Zhang, L.L. and Zhao, X.S. (2009), "Carbon-based materials as supercapacitor electrodes." *Chemical Society Reviews*, Vol. **38**, 2520-2531